Fast Preparation and Characterization of Quarternary Thermoelectric Clathrates

Mogens Christensen,† Simon Johnsen, Martin Søndergaard, Jacob Overgaard, Henrik Birkedal, and Bo B. Iversen*

Centre for Energy Materials, Department of Chemistry and iNANO, University of Aarhus, DK-8000 Århus C, Denmark

Received August 23, 2008. Revised Manuscript Received November 4, 2008

A large functionally graded single crystal has been synthesized by the Czochralski method. The resulting rod has a continuous composition range of $Ba_8Ga_{16}(Si_xGe_{1-x})_{30}$ going from $x = 0.20(1)$ to 0.41(1). The exact composition was determined along the pulling direction by energy-dispersive X-ray spectroscopy (EDX), synchrotron powder X-ray diffraction (PXRD), and single-crystal X-ray diffraction (SCXRD). Spatially resolved thermopower was measured using a Potential Seebeck Microprobe showing a gradual change in the thermopower with varying Si/Ge ratio. The gradual change is also observed in the clathrate lattice parameter. The present study demonstrates a method for fast preparation and characterization of a broad stoichiometry range in complex thermoelectric materials such as quarternary clathrate $Ba_8Ga_{16}(Si_xGe_{1-x})_{30}$. Furthermore, the method can potentially be used to produce functionally graded materials, which have thermoelectric properties optimized over a broad temperature range.

Introduction

The discovery of a series of promising host−guest materials in the midnineties led to a renewed interest in the field of thermoelectrics.[1−3] The materials are based on a design strategy coined the "phonon-glass-electron crystal" (PGEC) concept.[4] Briefly, a good thermoelectric material should conduct heat like an amorphous material and electricity like a crystal. The basic hypothesis is that a semiconducting host structure has a high thermopower (S) and electric conductivity (σ), whereas extreme thermal motion of loosely bound guest atoms located in cavities reduces the thermal conductivity (κ). This results in a large dimensionless thermoelectric figure of merit, $zT = TS^2\sigma/\kappa$. The outstanding property of the new materials is that they have a low lattice contribution to κ without degrading σ. The coupling between the vibrational energy of the guest atoms and the lattice phonons of the host structure can be manipulated by atomic scale engineering of the structure and chemical function of the cavity.[5,6]

One of the most promising new classes of materials is the clathrates, which consist of an open host framework with loosely bonded guest ions trapped in the cages, Figure 1. A large number of studies have focused on the guest-atom "rattling" in clathrates,[7−9] and clathrates have been developed with $zT > 1$.[10] Clathrates are extremely chemically stable and can be exposed to concentrated acid and aggressive atmospheres without a reduction of their performance.[10−13] The main hypothesis guiding the many research efforts on clathrates has been that low energy guest-atom vibrations hybridize with the acoustic phonons of the framework to

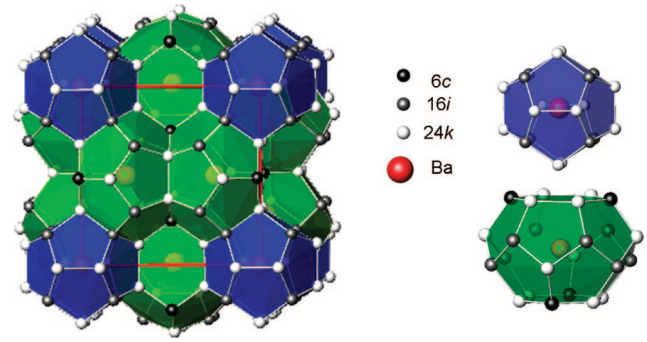

Figure 1. Crystal structure of $Ba_8Ga_{16}(Si_xGe_{1-x})_{30}$ is shown on the left. On the 2*a* site Ba is coordinated to 20 framework atoms (blue polyhedra) and on the 6*d* site to 24 atoms (green polyhedra). The Ga, Si, and Ge atoms are distributed over the three distinct lattice sites denoted 6*c*, 16*i*, and 24*k* (black, gray, and white spheres, respectively).

* To whom correspondence should be addressed. E-mail: bo@chem.au.dk.
† Current address: The Bragg Institute, ANSTO, NSW 2234 Menai, Australia.

(1) Morelli, D. T.; Meisner, G. P. *J. Appl. Phys.* **1995**, *77*, 3777–3781.
(2) Nolas, G. S.; Cohn, J. L.; Slack, G. A.; Schjuman, S. B. *Appl. Phys. Lett.* **1998**, *73*, 178.
(3) Snyder, G. J.; Toberer, E. S. *Nat. Mater.* **2008**, *7*, 105–114.
(4) Slack, G. A. *New Materials and Performance Limits for Thermoelectric Cooling*; Rowe, D. M., Ed.; CRC Handbook of Thermoelectrics; CRC Press: Boca Raton, FL, 1995; p 407.
(5) Christensen, M.; Juranyi, F.; Iversen, B. B. *Physica B* **2006**, *385*, 505–507.
(6) Suekuni, K.; Avila, M. A.; Umeo, K.; Takabatake, T. *Phys. Rev. B* **2007**, *75*, 195210.
(7) Cohn, J. L.; Nolas, G. S.; Fessatidis, V.; Metcalf, T. H.; Slack, G. A. *Phys. Rev. Lett.* **1999**, *82*, 779–782.
(8) Iversen, B. B.; Palmqvist, A. E. C.; Cox, D. E.; Nolas, G. S.; Stucky, G. D.; Blake, N. P.; Metiu, H. *J. Solid State Chem.* **2000**, *149*, 455–458.
(9) Sales, B. C.; Chakoumakos, B. C.; Jin, R.; Thompson, J. R.; Mandrus, D. *Phys. Rev. B* **2001**, *63*, 245113.
(10) Saramat, A.; Svensson, G.; Palmqvist, A. E. C.; Stiewe, C.; Mueller, E.; Platzek, D.; Williams, S. G.; Rowe, D. M.; Bryan, J. D.; Stucky, G. D. *J. Appl. Phys.* **2006**, *99*, 023708.
(11) Eisenmann, B.; Schäfer, H.; Zagler, R. *J. Less Common Met.* **1986**, *118*, 43–55.
(12) Cordier, G.; Woll, P. *J. Less Common Met.* **1991**, *169*, 291.
(13) Toberer, E. S.; Christensen, M.; Iversen, B. B.; Snyder, G. J. *Phys. Rev. B* **2008**, *77*, 075203.

10.1021/cm802289n CCC: $40.75
Published on Web 12/04/2008

lower the thermal conductivity.[7] It has been shown by means of triple axis spectroscopy that the guest atom causes flattening of the phonon dispersion modes, which lowers the phonon group velocity and effectively reduces the thermal conductivity.[14]

Recently, the efforts to optimize the clathrates have shifted from the guest atom toward the host structure.[15−20] It has for example been shown that slight changes in host structure composition in $Ba_8Al_{16-x}Ge_{30+x}$ fundamentally alters the nuclear density distribution of the guest atom.[20] Furthermore, it was found that changes in the host structure composition changes not only the electrical properties but also the thermal conductivity.[20] It appears that manipulation of the chemical composition of the host structure is the key to controlling the thermoelectric properties of clathrates. In addition the host structure can be influenced by substitution, thereby turning the samples into ternary and quaternary phases. A few examples of quaternary phases already exists in the literature; $Sr_8Ga_{16}Si_xGe_{30-x}$, $Ba_8Ga_{16}Si_xGe_{30-x}$, $Ba_8Ga_{16}Zn_xGe_{30-x}$, $Ba_8Ga_{16}Al_xGe_{30-x}$, and $Ba_8Ga_{16}Ge_{30}$ with substitution of In and Sb.[6,21−26] The efficiency of a thermoelectric material scales with zT, and individual evaluation of the three parameters, σ, S, and κ, is necessary to assess the thermoelectric performance of a given material.[27] Therefore, the investigation of the thermoelectric performance of ternary and quaternary solid solutions can rapidly become an insurmountable task.[28,29]

Here, we present a fast method for synthesizing and investigating a continuous range of compositions in a quaternary system. As a proof of concept a single crystal of $Ba_8Ga_{16}(Si_xGe_{1-x})_{30}$ with composition range x from 0.20(1) to 0.41(1) was pulled from a melt with nominal composition $Ba_8Ga_{16}(Si_{0.25}Ge_{0.75})_{30}$ in just ∼10 h. The continuous change of Si/Ge content gives variations in the structural and physical properties, and allows identification of the optimal substitution level. This way of producing quaternary systems is significantly faster than producing the samples one by one. The method also has a strong potential for producing functionally graded thermoelectric materials that have optimal performance over a broad temperature range, thus increasing the energy conversion efficiency. The element gradient and the related changes in the physical properties are investigated by local probe techniques, X-ray diffraction and bulk transport measurements.

Experimental Section

Synthesis. A large single crystal was pulled by the Czochralski method from a melt with nominal stoichiometry $Ba_8Ga_{16}(Si_{0.25}Ge_{0.75})_{30}$. The starting compounds of $Ba_8Ga_{16}Si_{30}$ and $Ba_8Ga_{16}Ge_{30}$ were synthesized separately by reacting stoichiometric quantities of pure elements. The presynthesized compounds were then mixed to produce the melt. The Czochralski pulling was performed in an induction furnace with an inert He atmosphere at an overpressure of ∼6 atm. A single crystal of $Ba_8Ga_{16}Si_{30}$ was attached to the upper shaft and used as seeding crystal. The crystal was pulled at a speed of 4.3 mm/h and resulted in a 53 mm long crystal with diameter of ∼8 mm. The resulting crystal was cut parallel to the pulling direction with a wire saw (Figure 2). For comparison single crystals of $Ba_8Ga_{16}Ge_{30}$ and $Ba_8Ga_{16}Si_{30}$ were also synthesized by the Czochralski method.

Physical Properties. Spatially resolved measurements of the room temperature thermopower were done using a PANCO Potential Seebeck Microprobe (PSM).[30] Grid point spacings of 50 and 100 μm were used. Samples for bulk measurements were cut at the places indicated by red boxes in Figure 2. Attention was paid to sample morphology to avoid cracks and fractures, which probably arise due to thermal stresses during cooling. The thermal transport properties were measured in a Quantum Design, Physical Properties Measurement System (PPMS). Conducting epoxy was used for mounting wires onto the samples. Resistivity was measured using a standard four point measurement. Thermal conductivity and thermopower were measured using the quasi steady-state method employed by the thermal transport option (TTO) for the PPMS.[31] Hall resistivity was measured on thin slabs ∼0.5 mm cut from the samples used for TTO measurements. Measurements in fields of $H = 0-9$ T in steps of 1 T at 10, 100, and 300 K were recorded at 0 and 180° to the perpendicular magnetic field in order to eliminate joule resistive errors. The resulting Hall resistivities were linear in field at all measured temperatures.

X-ray Diffraction and EDX. Samples for diffraction were filed off the pieces cut for the bulk transport measurements (indicated by red boxes in Figure 2). Single crystals with a diameter of ∼50 μm were used for single crystal X-ray diffraction on a Bruker APEX-II diffractometer using Mo Kα radiation. The temperature was held at 100 K using an Oxford cryostream device. Parts of the remaining sample were ground and used for high energy synchrotron powder X-ray diffraction at room temperature at BL02B2, SPring8, Japan.[32] Prior to the data collection the wavelength (λ = 0.357459(2) Å) was determined by refinement of data measured on a standard sample of CeO_2 (a = 5.411101 Å). Full site occupancy was assumed on all crystallographic sites in refinements

(14) Christensen, M.; Abrahamsen, A. B.; Christensen, N. B.; Juranyi, F.; Andersen, N. H.; Lefmann, K.; Andreasson, J.; Bahl, C. R. H.; Iversen, B. B. *Nat. Mater.* **2008**, *7*, 811–815.
(15) Bentien, A.; Palmqvist, A. E. C.; Bryan, J. D.; Latturner, S.; Stucky, G. D.; Furenlid, L.; Iversen, B. B. *Angew. Chem., Int. Ed.* **2000**, *39*, 3613–3616.
(16) Bentien, A.; Iversen, B. B.; Bryan, J. D.; Stucky, G. D.; Palmqvist, A. E. C.; Schultz, A. J.; Henning, R. W. *J. Appl. Phys.* **2002**, *91*, 5694–5699.
(17) Bentien, A.; Pacheco, V.; Paschen, S.; Grin, Y.; Steglich, F. *Phys. Rev. B* **2005**, *71*, 165206.
(18) Bentien, A.; Johnsen, S.; Iversen, B. B. *Phys. Rev. B* **2006**, *73*, 094301.
(19) Christensen, M.; Lock, N.; Overgaard, J.; Iversen, B. B. *J. Am. Chem. Soc.* **2006**, *128*, 15657–15665.
(20) Christensen, M.; Iversen, B. B. *Chem. Mater.* **2007**, *19*, 4896–4905.
(21) Martin, J.; Erickson, S.; Nolas, G. S.; Alboni, P.; Tritt, T. M.; Yang, J. *J. Appl. Phys.* **2006**, *99*, 044903.
(22) Martin, J.; Nolas, G. S.; Wang, H.; Yang, J. *J. Appl. Phys.* **2007**, *102*, 103719.
(23) Deng, S.; Tang, X.; Zhang, Q. *J. Appl. Phys.* **2007**, *102*, 043792.
(24) Deng, S.; Tang, X.; Zhang, Q. *J. Appl. Phys.* **2008**, *103*, 073503.
(25) Okamoto, N. L.; Kishida, K.; Tanaka, K.; Inui, H. *J. Appl. Phys.* **2007**, *101*, 113525.
(26) Latturner, S.; Bu, X.; Blake, N.; Metiu, H.; Stucky, G. *J. Solid State Chem.* **2000**, *151*, 61–64.
(27) Rowe, D. M. In *CRC Handbook of Thermoelectrics*; CRC Press: Boca Raton, FL, 1995; p 701.
(28) Mudryk, Y.; Rogl, P.; Paul, C.; Berger, S.; Bauer, E.; Hilscher, G.; Godart, C.; Noel, H. *J. Phys.: Condens. Matter* **2002**, *14*, 7991.
(29) Melnychenko-Koblyuk, N.; Grytsiv, A.; Rogl, P.; Rotter, M.; Lackner, R.; Bauer, E.; Fornasari, L.; Marabelli, F.; Giester, G. *Phys. Rev. B* **2007**, *76*, 195124.
(30) Platzek, D.; Karpinski, G.; Stiewe, C. ; Ziolkowski, P.; Drasar,C.; Müller, E. *Proceedings of the 24th International Conference on Thermoelectrics*; Tritt, T. M., Ed.; IEEE: Piscataway, NJ, 2005; p 13.
(31) Maldonado, O. *Cryogenics* **1992**, *32*, 908.
(32) Nishibori, E.; Takata, M.; Kato, K.; Sakata, M.; Kubota, Y.; Aoyagi, S.; Kuroiwa, Y.; Yamakata, M.; Ikeda, N. *Nucl. Instrum. Methods Phys. Res. A* **2001**, *467*, 1045.

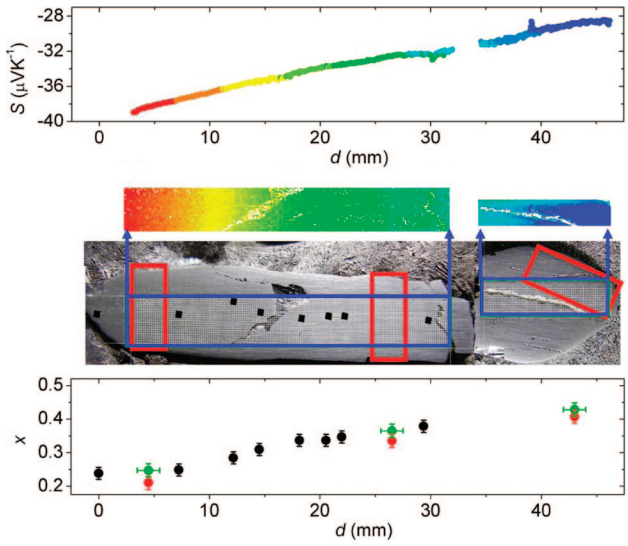

Figure 2. (Top) The graph shows the vertical line-average thermopower (S) as a function of the distance (d) extracted from the surface color plot below. The color scale refers to the value of the thermopower. (Middle) Picture of the sample, where the blue boxes indicate the areas for the potential Seebeck microprobe (PSM) measurements, which are shown in the upper picture. Red boxes give the positions from where samples for bulk measurements were cut and samples for diffraction analysis were extracted. Black squares correspond to areas for EDX measurements. (Bottom) Si content x in $Ba_8Ga_{16}(Si_xGe_{1-x})_{30}$ as a function of d. Black circles are EDX measurements corresponding to the spots in the middle picture. The red and green circles correspond to refined Si content from SCXRD and PXRD data, respectively.

of both the SCXRD data and the PXRD data. In the SCXRD refinements the Ga content was constrained to 16 Ga per formula unit, whereas for PXRD refinements the scattering properties of Ge was used for both Ge and Ga as the difference in scattering power at the used wavelength is small and negligible compared to the difference between Ga/Ge and Si. The SCXRD structural refinements were carried out using SHELX,[33] whereas the powder diffraction data were refined using Fullprof.[34] Differential scanning calorimetry (DSC) was measured on the remaining extracted sample using a Netzsch STA 449C Jupiter. Chemical analysis was carried out using energy-dispersive X-ray spectroscopy (EDX) on a Nova NanoSEM with an EDAX detector.

Results and Discussion

Synthesis. The higher melting point of $Ba_8Ga_{16}Si_{30}$ relative to $Ba_8Ga_{16}Ge_{30}$, causes Si rich $Ba_8Ga_{16}(Si_xGe_{1-x})_{30}$ to solidify first as the seeding crystal is pulled from the melt, however as the melt is depleted of Si the precipitating composition will have a continuously reduced Si concentration. In other words, a gradient in Si/Ge content arises along the pulling direction of the crystal.[35] The pulled single crystal has a composition of $Ba_8Ga_{16}(Si_xGe_{1-x})_{30}$ with x decreasing when going from top to the bottom of the sample.

Thermopower. Spatially resolved thermopower measurements along the crystal pulling axis are shown in Figure 2. A clear gradient is observed in the thermopower (S) ranging from from -29 μV K^{-1} at the top to -39 μV K^{-1} in the bottom part of the rod. Figure 3 shows the corresponding thermopower scan for a single crystal of pure $Ba_8Ga_{16}Ge_{30}$. A scan perpendicular to the pulling direction reveals $Ba_8Ga_{16}Ge_{30}$ to have a homogeneous thermopower depth profile. The perpendicular scan and a scan for $Ba_8Ga_{16}Si_{30}$ are included in the Supporting Information. The $Ba_8Ga_{16}Ge_{30}$ crystal has a homogeneous thermopower of $S = -53(1)$ μV K^{-1} throughout the crystal, whereas the thermopower of a Czochralski pulled $Ba_8Ga_{16}Si_{30}$ was found to be $-5(1)$ μV K^{-1} at room temperature. The variation in thermopower of the $Ba_8Ga_{16}(Si_xGe_{1-x})_{30}$ crystal is a combined effect of the Si/Ge gradient and the slight decrease in charge carrier concentration (see below) along the crystal pulling direction. A limitation of the thermopower scan is that it gives the thermopower only while the electrical and thermal conductivities still need to be measured by other methods to establish the thermoelectric figure of merit.

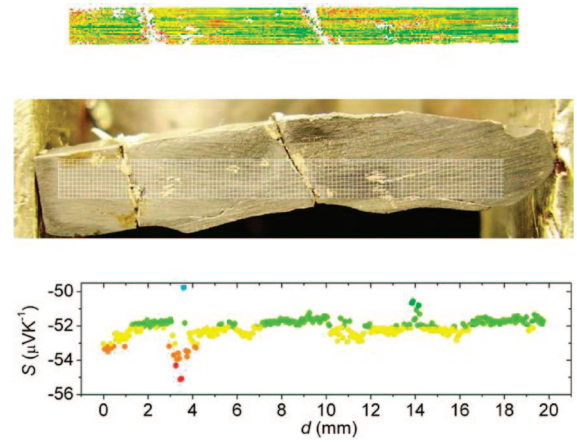

Figure 3. (Upper graph) Spatially resolved thermopower scan of the Czochralski pulled $Ba_8Ga_{16}Ge_{30}$ crystal shown in the middle picture. (Lower graph) Vertical mean value.

X-ray Diffraction and EDX. The observed gradient in Si/Ge content was confirmed by synchrotron powder and single crystal diffraction as well as the EDX analysis. Figure 2 (bottom) shows the Si content extracted from X-ray diffraction methods and EDX as function of the position in the sample. A Si/Ge element gradient is clearly visible along the pulling direction of the crystal. Similarly, though not statistically significant within the resolution of the EDX measurements there is a tendency for Ga content to increase along the length of the sample in agreement with the varying extrinsic contribution to the charge carrier concentration. The Si content estimated from EDX measurements is in good agreement with the results extracted from the X-ray diffraction data. In Table 1, the unit cell refined from room temperature synchrotron powder data and 100 K single crystal X-ray diffraction data are tabulated along with the site occupancy factors (sof) and the refined Si content x defined as $Ba_8Ga_{16}(Si_xGe_{1-x})_{30}$ (for complete listing of refined parameters see the Supporting Information). A systematic increase in the lattice parameter is found along the crystal pulling direction from top to bottom and simultaneously the refined Si content (x) decreases. This is evident from both the synchrotron powder (300 K) and the single crystal X-ray diffraction data (100 K). The refined Si contents, x, obtained from the single crystal and the powder data are in good

(33) Sheldrick, G. M. *SHELX*; Bruker AXS Inc.: Madison, WI, 2003.
(34) Rodriguez-Carvajal, J. *Fullprof* **2005**, *v3.20 Feb*, 2005.
(35) Pamplin, B. R. In *Crystal Growth; International Series of Monographs in the Science of the Solid State*; Pergamon press: Oxford, U.K., 1975; Vol. 6.

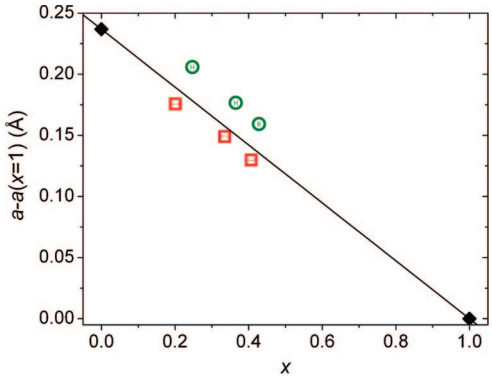

Figure 4. Normalized lattice parameter, $a - a(x = 1)$, versus refined Si content, where $x = 1$ corresponds to pure $Ba_8Ga_{16}Si_{30}$. The plot shows data for the top, middle, and bottom part of the crystal. Lattice parameters taken from Bentien *et al.* for $Ba_8Ga_{16}Ge_{30}$ and $Ba_8Ga_{16}Si_{30}$ are shown as black diamonds and included for comparison.[36] The red squares are from the SCXRD data (100 K), whereas the green spheres are from the PXRD data (300 K).

Table 1. Selected Refinement Details from Room-Temperature PXRD and 100 K SCXRD; Lattice Parameter (*a*), Site-Specific Si Occupancies, and the Total Fractional Si Content (*x*)

	param	top	middle	bottom
PXRD(RT)	*a* (Å)	10.68633(5)	10.70371(4)	10.73291(4)
	6*c*(Si%)	11.3(6)	11.3(6)	8.4(6)
	16*i*(Si%)	46.4(3)	39.2(3)	26.9(4)
	24*k*(Si%)	19.7(3)	16.7(4)	10.8(4)
	x	0.428(3)	0.365(4)	0.247(4)
SCXRD(100K)	*a* (Å)	10.6569(2)	10.6761(2)	10.70270(10)
	6*c*(Si%)	5.3(1.0)	7.8(1.1)	5.5(1.3)
	16*i*(Si%)	45.4(9)	37.0(9)	23.7(1.0)
	24*k*(Si%)	19.3(9)	15.3(9)	9.1(1.0)
	x	0.407(8)	0.335(9)	0.201(9)

agreement. Comparing the individual host structure sites it is observed that only the 6*c* site with low Si occupancy is showing a notable deviation between the powder and single crystal diffraction data. Si atoms are predominantly found at the 16*i* site followed by the 24*k* site. Both 16*i* and 24*k* are observed to decrease in Si content as the total content *x* decreases. In Figure 4 the unit cell parameter *a* is plotted as a function of *x*. Lattice parameters for stoichiometric $Ba_8Ga_{16}Ge_{30}$ and $Ba_8Ga_{16}Si_{30}$ have been added for comparison.[36] The lattice constants obtained from single crystal diffraction and synchrotron powder diffraction are showing the same systematic trends. The differences in absolute unit cells between the two are due to the difference in data collection temperature.

Physical Properties. The bulk transport properties measured as a function of temperature are shown in Figure 5. The room temperature thermopowers are -39 and -29 μV K^{-1} for the bottom and top sample, respectively, in excellent agreement with the spatially resolved thermopower scan. Within the resolution of the Hall measurements, no change was seen in the charge carrier concentration at the different measurement temperatures. For the top sample the charge carrier concentration amounts to $2.5(2) \times 10^{-21}$ cm^{-3}, whereas $1.0(1) \times 10^{-21}$ cm^{-3} is found for the bottom. Using a parabolic band model and the thermopower data this yields effective masses of $2.7(2)m_e$ and $2.0(1)m_e$ for the top and

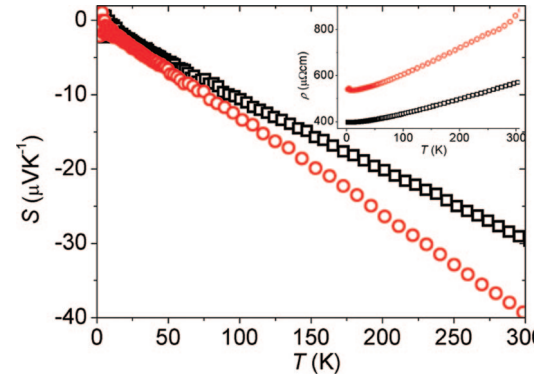

Figure 5. Electronic transport properties measured on the bulk samples cut from the top ($x = 0.4$, black squares) and the bottom ($x = 0.2$, red circles) of the crystal. The main graph shows the thermopower (*S*), whereas the resistivity (ρ) is shown in the inset.

bottom, respectively. Here, m_e is the free electron mass. For the top and bottom samples, Hall mobilities of 4.5(4) and 7.1(2) cm^2 V^{-1} s^{-1} are found. The lattice thermal conductivity (κ_L) is plotted in Figure 6 for $Ba_8Ga_{16}Si_{30}$, the top sample, the bottom sample, and $Ba_8Ga_{16}Ge_{30}$, where the subtracted electronic contribution has been estimated using Wiedemann–Franz's law with $L = 2.44 \times 10^{-8}$ W Ω K^{-2}. At low temperatures, where Rayleigh scattering is dominant compared to Umklapp processes, another effect of the Si content in the samples is apparent. Rayleigh scattering has several contributions, notably scattering on impurities, imperfections, and mass difference. Considering the latter, then to a first approximation the phonon mean free path becomes inversely proportional to $g = \sum_{i,j} n_{ij}(1 - m_{ij}/M_j)^2$ where n_{ij} is the volume density of the *i*th element at the *j*th site, m_{ij} is the atomic mass of the *i*th element at the *j*th site, and M_j is the mean mass of the atoms at the *j*th site.[36] The phonon mean free path and consequently the thermal conductivity scales inversely with the mass difference. The mass difference between the light Si and heavier almost equal masses of Ga and Ge causes a significant mass variation. The decrease in Si increases the thermal conductivity at temperatures well below the Debye temperature,[37] and indeed the low temperature peak in κ_L is reduced with increasing Si content.

Differential Scanning Calorimetry. The melting point measured by differential scanning calorimetry (DSC) increases with increasing *x*. This is expected as the stoichiometric compounds $Ba_8Ga_{16}Ge_{30}$ and $Ba_8Ga_{16}Si_{30}$ have melting points of 1236(5) and 1453(5) K, respectively. The result is another independent verification of the Si/Ge gradient in the sample and a textbook example of crystal growth from a solid solution; see the Supporting Information for further details.

Discussion

Synthesis. Experimental and theoretical work has recently been reported for the solid solutions of $Sr_8Ga_{16}(Si_xGe_{1-x})_{30}$ and $Ba_8Ga_{16}(Si_xGe_{1-x})_{30}$.[6,21,22,38] Polycrystalline samples of

(36) Bentien, A.; Nishibori, E.; Paschen, S.; Iversen, B. B. *Phys. Rev. B* **2005**, *71*, 144107.
(37) Ziman, J. M. In *Electrons and Ponons. The Theory of Transport Phenomena in Solids*;Claredon Press: Oxford, U.K., 2001.
(38) Nenghabi, E. N.; Myles, C. W. *Phys. Rev. B* **2008**, *77*, 205203.

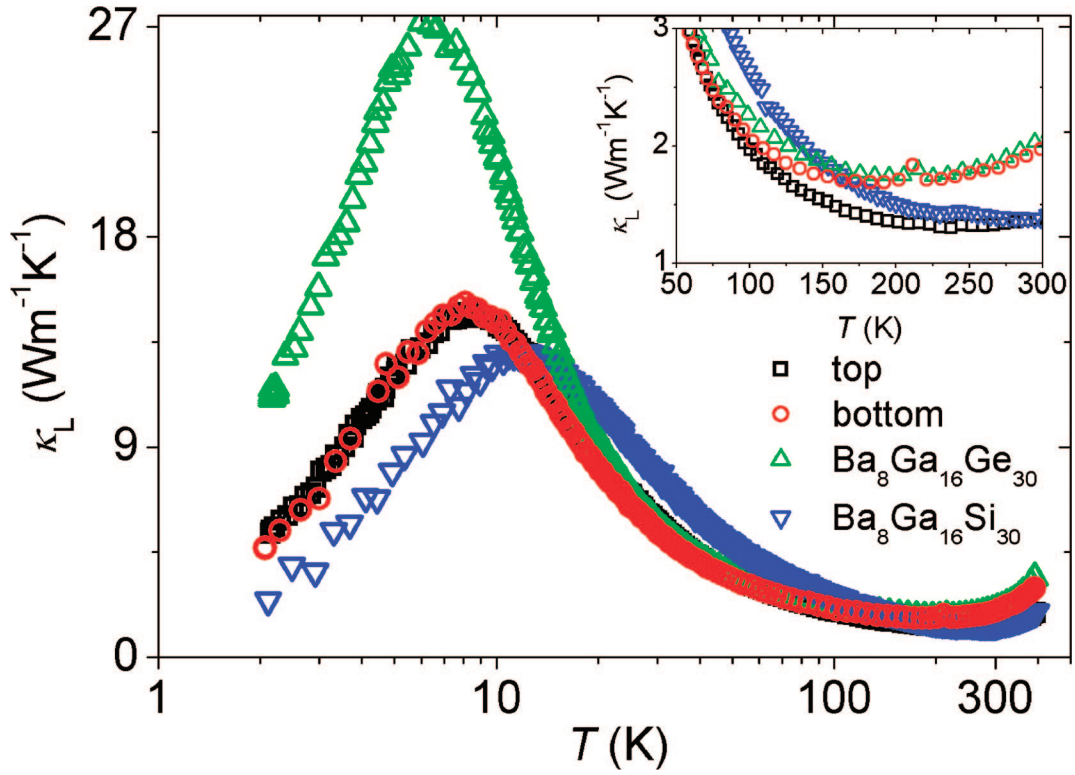

Figure 6. Lattice thermal conductivity (κ_L) of the bulk samples cut from the bottom (red circles) and top (black squares) part of the crystal. $Ba_8Ga_{16}Ge_{30}$ (green triangles) and $Ba_8Ga_{16}Si_{30}$ (blue triangles) are shown for comparison. The inset shows the lattice thermal conductivity at high temperatures. The $Ba_8Ga_{16}Ge_{30}$ and the bottom samples have large surface to volume ratios since they were cut very thinly to aviod cracks. Hence both samples show upturning tails due to thermal radiation above ~100 K.

$Ba_8Ga_{16}(Si_xGe_{1-x})_{30}$ were reported in two papers describing different x ranges. The first paper reported on the range $0 < x < 0.17$,[21] whereas the second paper has an extended range $0.13 < x < 0.45$.[22] The ranges are comparable to our results obtained by the Czochralski method $0.2 < x < 0.4$. The polycrystalline samples of the first paper were prepared by solid state reaction of stoichoimetric quantities and in the second paper Si and Ge were prereacted before mixing with Ba and Ga. The first preparation method resulted in significant Si impurity above $x > 0.2$.[21] The second synthesis route gave trace impurities of Si, Ge and Si−Ge alloy with concentrations of up to 4 vol %.[22] The Czochralski method provided phase pure sample within the resolution of the powder synchrotron data, i.e., better than 0.05 vol %. Hence the encountered problems of sample porosity, morphology, and impurities with polycrystalline samples are avoided in the present approach, which consequently provide a faster and improved method to investigate complex phases. Unfortunately, variations in the charge carrier concentration appear unavoidable in the present system, but the present variations are similar to the relative variations reported in the papers by Martin et al.[21,22] To a certain extent the variation in the charge carrier concentration obscures the effect of the Si/Ge gradient in the thermopower whereas properties related to the crystal structure, e.g., lattice parameters and lattice thermal conductivity are unaffected.

X-ray Diffraction. Martin et al. assumed the Si atoms to primarily occupy the 6*c* site,[21] however this disagrees with the present result, where Si preferably occupies the 16*i*, 24*k*, and 6*c* sites in that order (see Table 1). Other studies have revealed that Ga and other low valence atoms prefer the 6*c* site.[19,20] In refinements of occupancies the discrepancy could be explained by vacancies, because Si is a weak scatterer in comparison with Ge and therefore vacancies can be modeled as a high Si content. Vacancies on the 6*c* site is likewise supported by the relative high sample porosity of the polycrystalline samples (81−85% of theoretical X-ray density).[21] Furthermore, vacancies are known to occur at the 6*c* site.[39,40] Ordered vacancies on the 6*c* site have been reported to form 2 × 2 × 2 superstructures and ordering of the Si distribution could possibly cause a superstructure, but no satellite peaks were observed in the single-crystal diffraction patterns.[41,42]

Physical Properties. The electrical resistivity reported by Martin et al. shows semiconducting behavior with decreasing resistivity with increasing Si content.[21,22] The present samples also have slight decrease in resistivity with increasing Si content, but the samples have metallic behavior, see insert in Figure 5. The thermopowers of the samples presented by Martin et al. go through an extreme for $x = 0.3$. In the present study, the thermopower clearly decreases continuously with increasing Si content and increasing extrinsic charge carrier contribution. Our findings are in good agreement with the values obtained from the end member compounds

(39) Carrillo-Cabrera, W.; Cardoso Gil, R.; Paschen, S. Grin, Yu. *Z. Kristallogr.* **2002**, *217*, 183–185.
(40) Melnychenko-Koblyuk, N.; Grytsiv, A.; Fornasari, L.; Kaldarar, H.; Michor, H.; Röhrbacher, F.; Koza, M.; Royanian, E.; Bauer, E.; Rogl, P.; Rotter, M.; Schmid, H.; Marabelli, F.; Devishvili, A.; Doerr, M.; Giester, G. *J. Phys.: Condens. Matter* **2007**, *19*, 216223.
(41) Carrillo-Cabrera, W.; Budnyk, S.; Prots, Y.; Grin, Y. *Z. Anorg. Allg. Chem.* **2004**, *630*, 2267–2276.
(42) Dubois, F.; Fässler, T. F. *J. Am. Chem. Soc.* **2005**, *127*, 3264–3265.

Table 2. Thermopower (S), Electrical Resistivity (ρ), Hall Charge Carrier Concentration (n_H), Band Effective Mass of the Charge Carriers in Units of the Free Electron Mass (m^*), and the Hall Charge Carrier Mobility (μ_H) of the Top and Bottom Sample; The Properties of Czochralski Pulled $Ba_8Ga_{16}Si_{30}$ and $Ba_8Ga_{16}Ge_{30}$ are Given for Comparison

	S (μV K^{-1})	ρ ($\mu\Omega$ cm)	n ($\times 10^{-21}$ cm^{-3})	m^* (m_e)	μ_H (cm^2 V^{-1} s^{-1})
$Ba_8Ga_{16}Si_{30}$	5(2)	331(1)	NA	NA	NA
top	29(2)	568(1)	2.5(2)	2.7(2)	4.5(4)
bottom	39(2)	861(1)	1.02(5)	1.97(6)	7.1(2)
$Ba_8Ga_{16}Ge_{30}$	53(2)	878(1)	0.493(5)	1.64(8)	14.5(9)

$Ba_8Ga_{16}Si_{30}$ ($S \approx -5\ \mu$V/K) and $Ba_8Ga_{16}Ge_{30}$ ($S \approx -50\ \mu$V/K). Martin et al. explains their observations by strong modification of the band curvature due to Si substitution.[21,22] This is corroborated by the present study where the band effective mass increases markedly with increasing Si content (see Table 2). However, contrary to the findings of Martin et al. the band effective masses are larger than the free electron mass and the effective mass in $Ba_8Ga_{16}Ge_{30}$. Vis à vis the change in band effective mass, it seems safe to partly relate the changes in the thermopower to the changes in the group IV element gradient, though the varying charge carrier contribution undoubtedly also has a pronounced effect.

The low-temperature peak in the thermal conductivity observed for crystalline materials is suppressed for the polycrystalline samples with substitution range between $0.1 < x < 0.2$,[21] whereas the samples with the substitution range $0.15 < x < 0.45$ clearly reveals the peak between 20 and 30 K,[22] although without any noticeable difference between the samples. The samples reported in the present paper reveal variation in the magnitude of the peak in the thermal conductivity, and our observations are in agreement with expectations from mass difference scattering (see the Supporting Information). The discrepancy between the thermal conductivity reported by Martin et al. and the samples reported in this paper is most likely due to imperfections and impurity scattering in the polycrystalline samples. Impurities and grain boundary scattering will reduce the main free path of the phonons and obscure the effect of mass difference scattering. This is also reflected by value of the thermal conductivity at the peak. Martin et al. find a thermal conductivity of about 3 W/(m K), whereas our samples have the thermal conductivity ranging from about 25 to 12 W/(m K).

For $Sr_8Ga_{16}(Si_xGe_{1-x})_{30}$ Suekuni et al. found a continuous solid solution and the properties were investigated for $x = 0$, 0.133, 0.333, 0.833, and 1.[6] Decreasing Si content was observed to cause suppression of the crystalline peak in the lattice thermal conductivity at ~15 K. The authors attributed this to the increasing free space of Sr as x decreases leading to enhanced resonance scattering by Sr. This is in contrast to the present study of $Ba_8Ga_{16}(Si_xGe_{1-x})_{30}$, where decreasing Si content causes an increase in the lattice thermal conductivity at around 8−15 K despite an increasing Ba free space. The difference between $Sr_8Ga_{16}(Si_xGe_{1-x})_{30}$ and $Ba_8Ga_{16}(Si_xGe_{1-x})_{30}$ can be explained by the difference in ionic radii between Sr and Ba, where the larger Ba fits more tightly in the clathrate cage. This means that the influence of resonance scattering is smaller for $Ba_8Ga_{16}(Si_xGe_{1-x})_{30}$ than for $Sr_8Ga_{16}(Si_xGe_{1-x})_{30}$. The thermal conductivity data clearly suggests that resonance scattering is less important at 15 K for the $Ba_8Ga_{16}(Si_xGe_{1-x})_{30}$ system relative to the aforementioned Rayleigh scattering. The observation of differences between $Sr_8Ga_{16}(Si_xGe_{1-x})_{30}$ and $Ba_8Ga_{16}(Si_xGe_{1-x})_{30}$ in the major phonon scattering mechanism at low temperature is important because these systems are often discussed on an equal footing creating apparent discrepancies. Regarding the electric resistivity and Seebeck coefficient for $Sr_8Ga_{16}(Si_xGe_{1-x})_{30}$ the increasing Si content decreases the resistivity and reduces the absolute value of the Seebeck coefficient. These trends are in agreement with our findings for $Ba_8Ga_{16}(Si_xGe_{1-x})_{30}$.

Conclusions

Because of the vast composition range in ternary and quaternary solid solutions, complete characterization of chemical and physical properties becomes an overwhelming task with conventional synthesis methods for bulk thermoelectric materials. There is an urgent need for faster and smarter screening methods. From a melt with nominal composition $Ba_8Ga_{16}(Si_{0.25}Ge_{0.75})_{30}$ a single crystal was pulled in just ~10 h using the Czochralski method resulting in a continuous stoichiometry of $Ba_8Ga_{16}(Si_xGe_{1-x})_{30}$ with $0.2 < x < 0.4$. The stoichiometric range covered by the crystal can be controlled by manipulating the initial melt composition and the dimensions of the pulled crystal. The method potentially has a wide applicability and many complex systems can be investigated rapidly. The clathrate type I structure offers numerous substitution possibilities by replacing Ge with Si and Sn, whereas Ga can be replaced by elements from the groups 10, 11, 12, and 13. It is clear that the spatially resolved thermopower measurement method is a powerful tool in the search for improved thermoelectric materials in quarternary systems. Furthermore, through control over the extrinsic contribution to the charge carrier concentration graded materials can be made, where the local zT value is optimized at the temperature of operation increasing the overall conversion efficiency. Because a wide composition range can be produced in the same crystal, materials optimized over a broad temperature range are within reach.

Acknowledgment. The Danish Research Councils and the Carlsberg Foundation are thanked for financial support. The synchrotron radiation experiments were performed at SPring-8 with the approval of the Japan Synchrotron Radiation Research Institute (JASRI). Dr. Eiji Nishibori is thanked for assistance during measurements.

Supporting Information Available: Photographs of the crystal, plot of the mass difference factor (g), powder diffraction patterns, full crystallographic refinement details, melting points from DSC measurements and Seebeck microprobe measurements of $Ba_8Ga_{16}Ge_{30}$ and $Ba_8Ga_{16}Si_{30}$ (PDF).This material is available free of charge via the Internet at http://pubs.acs.org.

CM802289N